



# A prototrophic suppressor of a *Vibrio fischeri* D-glutamate auxotroph reveals a member of the periplasmic broad-spectrum racemase family (BsrF)

Macey N. Coppinger,<sup>1,2</sup> Kathrin Laramore,<sup>1</sup> David L. Popham,<sup>3</sup> Eric V. Stabb<sup>2</sup>

**AUTHOR AFFILIATIONS** See affiliation list on p. 14.

**ABSTRACT** Although bacterial peptidoglycan (PG) is highly conserved, some natural variations in PG biosynthesis and structure have evolved. Understanding the mechanisms and limits of such variation will inform our understanding of antibiotic resistance, innate immunity, and the evolution of bacteria. We have explored the constraints on PG evolution by blocking essential steps in PG biosynthesis in *Vibrio fischeri* and then selecting mutants with restored prototrophy. Here, we attempted to select prototrophic suppressors of a D-glutamate auxotrophic *murl racD* mutant. No suppressors were isolated on unsupplemented lysogeny broth salts (LBS), despite plating  $>10^{11}$  cells, nor were any suppressors generated through mutagenesis with ethyl methanesulfonate. A single suppressor was isolated on LBS supplemented with iso-D-gln, although the iso-D-gln subsequently appeared irrelevant. This suppressor has a genomic amplification formed by the creation of a novel junction that fuses *proB* to a gene encoding a putative broad-spectrum racemase of *V. fischeri*, *bsrF*. An engineered *bsrF* allele lacking the putative secretion signal ( $\Delta SS$ -*bsrF*) also suppressed D-glu auxotrophy, resulting in PG that was indistinguishable from the wild type. The  $\Delta SS$ -*bsrF* allele similarly suppressed the D-alanine auxotrophy of an *alr* mutant and restored prototrophy to a *murl alr* double mutant auxotrophic for both D-ala and D-glu. The  $\Delta SS$ -*bsrF* allele increased resistance to D-cycloserine but had no effect on sensitivity to PG-targeting antibiotics penicillin, ampicillin, or vancomycin. Our work helps define constraints on PG evolution and reveals a periplasmic broad-spectrum racemase in *V. fischeri* that can be co-opted for PG biosynthesis, with concomitant D-cycloserine resistance.

**IMPORTANCE** D-Amino acids are used and produced by organisms across all domains of life, but often, their origins and roles are not well understood. In bacteria, D-ala and D-glu are structural components of the canonical peptidoglycan cell wall and are generated by dedicated racemases Alr and Murl, respectively. The more recent discovery of additional bacterial racemases is broadening our view and deepening our understanding of D-amino acid metabolism. Here, while exploring alternative PG biosynthetic pathways in *Vibrio fischeri*, we unexpectedly shed light on an unusual racemase, BsrF. Our results illustrate a novel mechanism for the evolution of antibiotic resistance and provide a new avenue for exploring the roles of non-canonical racemases and D-amino acids in bacteria.

**KEYWORDS** Photobacterium, *Aliivibrio*, D-amino acids, peptidoglycan, broad-spectrum racemase, D-glutamate, racemase

Most bacteria have a cell wall comprised of peptidoglycan (PG), which helps define cell shape and provides resilience against environmental stresses. As a highly conserved and uniquely bacterial structure, PG is a key microbe-associated molecular

**Editor** Michael Y. Galperin, NCBI, NLM, National Institutes of Health, Bethesda, Maryland, USA

Address correspondence to Eric V. Stabb, estabb@uic.edu.

The authors declare no conflict of interest.

See the funding table on p. 14.

**Received** 8 December 2023

**Accepted** 4 February 2024

**Published** 27 February 2024

Copyright © 2024 American Society for Microbiology. All Rights Reserved.

pattern recognized by bacteria-surveillance systems of plants and animals and is a prime target for medically relevant antibiotics. Although PG and its biosynthesis are strikingly similar across the bacterial kingdom, PG structural variations have evolved (1). Understanding the possible trajectories for and constraints on PG evolution will inform our understanding of host–microbe interactions and the emergence of resistance to PG-targeting antibiotics.

We became interested in PG in *Vibrio fischeri* because of PG's role in the symbiosis between *V. fischeri* and the Hawaiian bobtail squid *Euprymna scolopes* (2–4). Specifically, PG monomers released by *V. fischeri* trigger the development of the host's symbiotic light organ (5–7). However, studying PG in *V. fischeri* is broadly relevant, as the PG structure and biosynthesis in *V. fischeri* parallel that in other Proteobacteria. For example, PG monomers released by *V. fischeri* are identical to tracheal cytotoxin and peptidoglycan cytotoxin released by *Bordetella pertussis* (8) and *Neisseria gonorrhoea* (9), respectively. Therefore, we have used *V. fischeri* as a model for exploring how bacteria can evolve new PG biosynthetic pathways. Our approach has been to block wild-type PG biosynthesis and select suppressor mutants capable of growing without a normally essential gene.

The *murl* gene contributes to PG biosynthesis and is considered essential in many bacteria (10, 11), including *V. fischeri* (12, 13). Murl is a cytoplasmic, pyridoxal phosphate-independent glutamate racemase that interconverts L- and D-glutamate, producing the D-glu for the peptide moiety of PG (14). Another cytoplasmic enzyme, MurD, adds D-glu to the second position of the PG peptide chain, linking it to the L-ala in the first position; then, MurE links the D-glu side chain acid to the amino group of DAP, creating gamma-D-glu (15). Glutamine has been found in the second position in a few bacteria, but in these cases, D-glu appears to be initially added by MurD, then later modified to iso-D-gln (16). Given their respective roles in an essential and uniquely bacterial pathway, both Murl and MurD have been considered as attractive antibacterial targets (17).

Previously, we generated a *murl* mutant in *V. fischeri* that, like *murl* mutants in other bacteria, could only be grown in media supplemented with D-glu (13). Subsequently, we selected prototrophic suppressors of this *murl* mutant that were able to grow without D-glu supplementation, leading to the discovery of a locus in *V. fischeri* and some other Proteobacteria that enables the catabolism of D-aspartate, underpinned by the aspartate racemase RacD (18). The overexpression of RacD could compensate for the loss of *murl*, with PG still containing D-glu, suggesting that RacD has glutamate racemase activities that can compensate for the loss of *murl* (18).

Here, the goal was to select suppressors of a *murl racD* mutant that have restored prototrophy. Such suppressors may create a new pathway to wild-type PG and/or evolve an altered PG structure. Aside from Murl and RacD, *V. fischeri* possesses a typical alanine racemase Alr, which provides the D-ala for PG. In other bacteria, Alr acts mostly on alanine and, to a lesser extent, serine (19). Due to its specificity for small, uncharged amino acids, it seemed unlikely that Alr would be involved in the suppression of D-glu auxotrophy without compromising D-ala production, although such a scenario could not be ruled out. It is also worth noting that MurD has a high specificity for D-glu as the substrate added to the PG peptide, but it is not known whether altered substrate specificity could obviate the need for D-glu. Although this background knowledge provides some important context for our selection, it was impossible to predict how or even if D-glu auxotrophy of a *murl racD* mutant could be suppressed.

## RESULTS

### Reversion of a *murl::mini-Tn5* allele by precise mini-transposon deletion

We first attempted to generate prototrophic suppressor mutants of RMJ13 (*murl::mini-Tn5 ΔracD*) by growing the strain in lysogeny broth salts (LBS) supplemented with D-glu, then plating the cells onto unsupplemented LBS. Mutants that grew independently of D-glu supplementation arose at a rate of  $\sim 10^{-10}$ ; however, whole genome sequencing of six prototrophs revealed that they were revertants at the *murl* locus. Instead of acquiring mutations at other sites to suppress D-glu auxotrophy, these strains had precisely

lost the mini-Tn5 transposon that had disrupted *murl*, reverting to a wild-type *murl* allele. The mini-Tn5 used encodes resistance to erythromycin (Em), and we subsequently determined that an additional 27 prototrophs selected in this manner were sensitive to Em, suggesting a similar loss of the mini-Tn5. Thus, instead of suppressing auxotrophy, these strains had reverted to prototrophic  $\Delta racD$  strains. Based on these data, the precise deletion of this mini-transposon, which does not encode a transposase (20), occurs at a rate of around  $10^{-10}$  (Table 1).

### Selection of a rare suppressor of D-glu auxotrophy

Further attempts to select suppressors in RMJ13 were performed with Em in the medium as a selective agent to maintain the transposon insertion in *murl*. However, after plating over  $10^{11}$  cells onto LBS-Em, we did not recover any suppressor mutants. Next, we performed a series of experiments chemically mutagenizing RMJ13 with ethyl methane-sulfonate (EMS), which primarily causes G:C to A:T transition mutations in DNA (21, 22). We plated a total of over  $10^8$ ,  $4 \times 10^7$ , and  $1.4 \times 10^7$  viable cells from treatments with approximately 90%, 99%, and 99.9% EMS-mediated killing, respectively, but still recovered no prototrophic suppressors of D-glu auxotrophy (Table 1).

We considered the possibility that supplements to LBS other than D-glu might allow us to select suppressors of D-glu auxotrophy. For example, knowing that D-glu is added to the PG side chain as iso-D-glu, we supplemented LBS-Em with iso-D-glutamine. From over  $10^{10}$  cells plated to LBS-Em with iso-D-gln, we selected one suppressor mutant, named RMJ13S10 (Table 1). Unexpectedly, subsequent experiments revealed that RMJ13S10 grew well on LBS-Em and does not require iso-D-gln supplementation (Fig. 1). Taken together, these results suggest that a rare mutation underpinned the suppression of D-glu auxotrophy in RMJ13S10, enabling it to grow on unsupplemented LBS.

### Mutation of *bsrF* suppresses D-glu auxotrophy

The genomic sequence of RMJ13S10 revealed an amplification of a 9.2-kb region in chromosome I spanning *bsrF* (VF\_0735) to *proB* (VF\_0740), including a novel fusion junction involving *proB* and *bsrF* (Fig. 2). In contrast to the wild-type sequence (Fig. 2A), the fusion disrupts the final five codons at the 3' end of *proB* and the start codon of *bsrF*. Those six amino acids are then replaced by a single valine, linking the two proteins together to create a fusion with an N-terminal ProB domain and C-terminal BsrF domain (Fig. 2B). Based on the relative number of sequencing reads, the 9.2-kb region appears to be amplified four to five times, relative to the surrounding regions. One would expect such a large amplification to be unstable and prone to reversion by homologous

TABLE 1 Selection for prototrophic suppressors in D-glu auxotroph RMJ13

| RMJ13 transposon revertants (LBS without Em) |                       |                      |                       |
|--|-----------------------|----------------------|-----------------------|
|  | CFU plated            | Revertants           | Revertants/CFU        |
| LBS  | $1.8 \times 10^{11}$  | 27                   | $1.4 \times 10^{-10}$ |
| RMJ13 EMS mutagenesis                        |                       |                      |                       |
|  | Plated                | Suppressors          | Suppressors/CFU       |
| 90% killing                                  | $1 \times 10^8$       | 0                    | — <sup>a</sup>        |
| 99% killing                                  | $4 \times 10^7$       | 0                    | —                     |
| 99.9% killing                                | $1.4 \times 10^7$     | 0                    | —                     |
| Total CFU plated                             |                       | $1.5 \times 10^8$    |                       |
| RMJ13 suppressor generation (LBS + Em)       |                       |                      |                       |
|  | Plated                | Suppressors          | Suppressors/CFU       |
| None   | $1.08 \times 10^{11}$ | 0                    | —                     |
| Iso-D-gln                                    | $1.13 \times 10^{10}$ | 1                    | $9 \times 10^{-11}$   |
| Total cells plated                           |                       | $1.4 \times 10^{11}$ |                       |

<sup>a</sup>— indicates below the limit of detection, i.e., no suppressors.

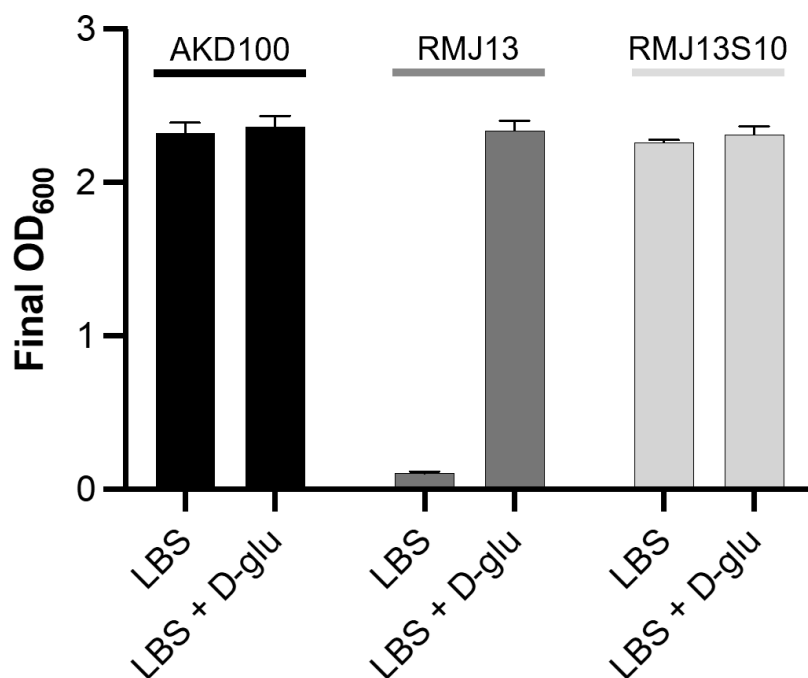


**FIG 1** D-glu independent prototrophy of suppressor RMJ13S10. Shown are final optical density at 600 nm ( $OD_{600}$ ) readings for *V. fischeri* cultures grown with or without 400  $\mu\text{g}/\text{mL}$  D-glu in LBS-Em. Strains include AKD100 (wild-type E5114 marked with Em resistance cassette at a neutral site), RMJ13 (*murl::mini-Tn5-erm  $\Delta$ racD*), and RMJ13S10 (*murl::mini-Tn5-erm  $\Delta$ racD proB-bsrF* fusion and amplification). Cultures were grown for 24 hours before reading the final  $OD_{600}$ . Error bars indicate the standard error of the mean ( $n = 8$ ). Data from one representative experiment of at least three are shown.

recombination under non-selective conditions. To test this genetic model, RMJ13S10 was grown in the absence of selective pressure (i.e., in LBS-Em supplemented with D-glu). By the fifth passage in non-selective culture, 30%–35% of CFUs had lost the ability to grow without D-glu supplementation (Fig. 2C) and had lost the *proB-bsrF* fusion (Fig. 2D and E).

The *bsrF* gene encodes a putative broad-spectrum racemase that shares 57% identity to the periplasmic BsrV characterized in *Vibrio cholerae* (19, 23–27). A bioinformatic analysis of the wild-type *V. fischeri* BsrF strongly suggested that the first 20 amino acids constitute a type-II Sec-dependent secretion signal, followed immediately by a cleavage site (Fig. 3A) (28). This amino acid stretch resembles the basic N-hydrophobic-C pattern seen in many signal peptides recognized by the Sec translocon system, and it has the typical signal sequence motif of having small, uncharged residues in positions  $-1$  and  $-3$  relative to the cleavage site (28). Thus, *in silico* analysis is consistent with BsrF secretion to the periplasm, like that of its ortholog in *V. cholerae*. When the ProB-BsrF fusion sequence was analyzed, however, no such secretion signal was found, which is unsurprising considering that the N-terminus of the fusion is ProB, a cytoplasmic protein.

We hypothesized that the ability of RMJ13S10 to suppress D-glu auxotrophy was due to the fusion of the cytoplasmic ProB to the periplasmic BsrF, burying the latter's secretion signal within the protein. This hypothesis proposes that fusion to ProB blocks BsrF secretion, allowing its racemase activity to compensate for the lack of Murl and RacD in the cytoplasm, where *de novo* PG synthesis occurs. To test this hypothesis, we generated a mutant *bsrF* allele that lacks the putative secretion signal sequence ( $\Delta$ SS-*bsrF*) (Fig. 3B). The  $\Delta$ SS-*bsrF* allele was then cloned into a shuttle vector (pVSV105) and introduced *in trans* into various *V. fischeri* strains. When placed in RMJ13, the  $\Delta$ SS-*bsrF* allele on pMNC26 fully suppressed D-glu auxotrophy, while pKAL6 carrying wild-type *bsrF* and the parent vector pVSV105 did not (Fig. 3C).

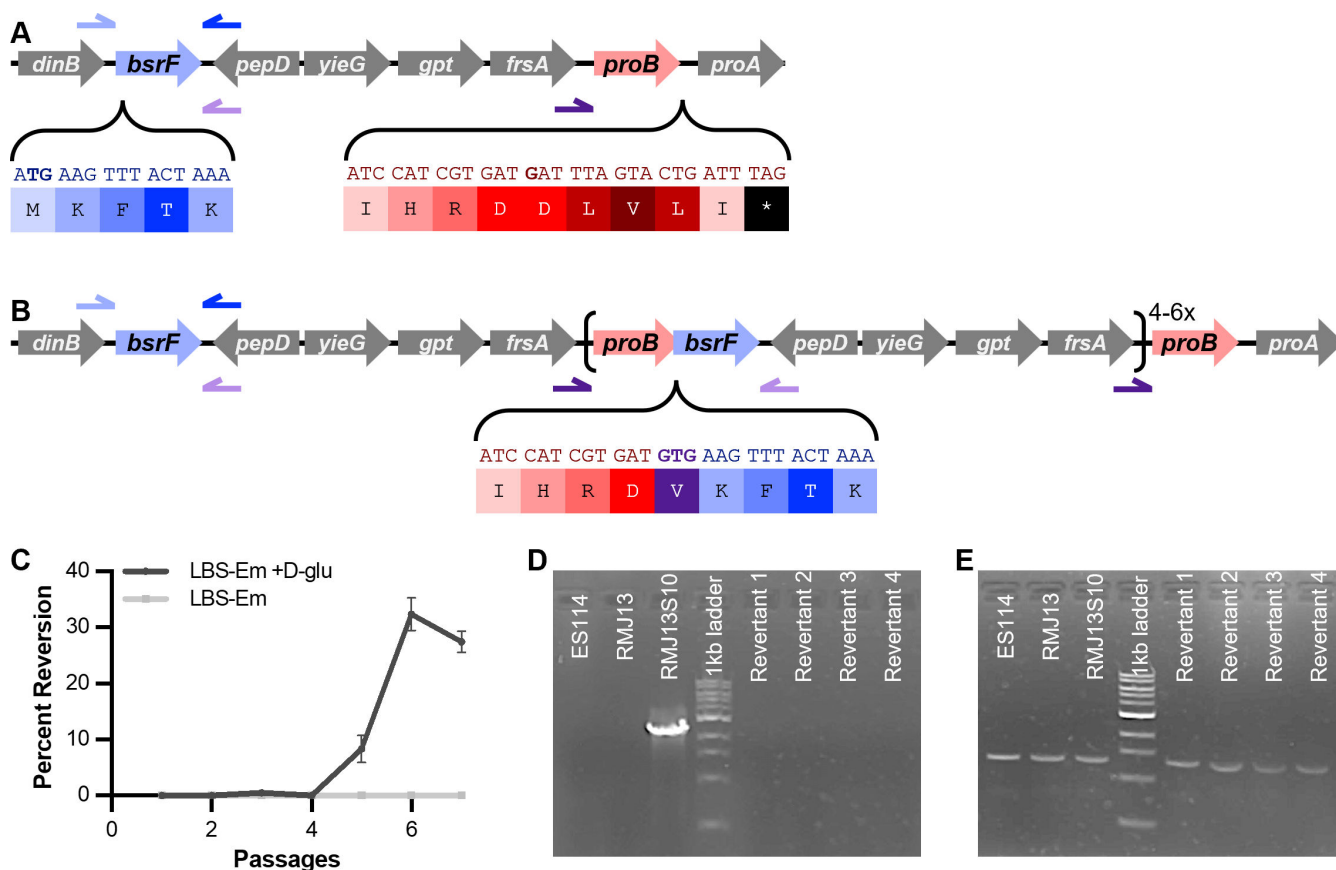


**FIG 2** Genotype of RMJ13S10. (A) Schematic of wild-type *V. fischeri* ES114 genotype, in the region containing *dinB* to *proA* (VF\_0734 to VF\_0741). Insets highlight the N-terminal region of *bsrF* and the C-terminal region of *proB*. Bases in bold are those encoding the newly created junction codon. Black arrows point to the spot where the original genetic sequences are fused in a novel junction. Blue arrows represent primers used to amplify wild-type *bsrF* (MC22 + MC23). Purple arrows represent primers used to amplify the *proB*-*bsrF* fusion (MC37 + MC38). (B) Schematic of the genetic fusion found in *V. fischeri* strain RMJ13S10. Brackets surround the genes that appear to be amplified. The inset highlights the new junction created by fusing *bsrF* to *proB*. Blue arrows represent primers used to amplify wild-type *bsrF*, and purple arrows represent primers used to amplify the *proB*-*bsrF* fusion. (C) When grown without selective pressure, the RMJ13S10 culture begins reverting to D-glu auxotrophy after multiple passages (for each passage, a stationary-phase culture was diluted 1:1,000 into fresh medium and grown for 24 hours). (D) 0.8% agarose gel with PCR products amplifying the *proB*-*bsrF* genetic fusion, which is present in RMJ13S10 but absent in revertants to D-glu auxotrophy. (E) 0.8% agarose gel with PCR products amplifying wild-type *bsrF*.

### Expression of $\Delta$ SS-BsrF increases resistance to D-cycloserine

We hypothesized that the cytoplasmic BsrF in RMJ13S10 might confer different patterns of resistance to antibiotics that act upon the cell wall, PG synthesis, or D-amino acid production. We found that this mutant's sensitivity to beta-lactams ampicillin and penicillin, as well as vancomycin, is similar to that of the wild type (data not shown); however, RMJ13S10 had increased resistance to D-cycloserine (DCS) relative to an Em-resistant derivative of the wild type (Fig. 4A). As noted below, DCS can inhibit the cytoplasmic alanine racemase *Alr*, and it seemed likely that the *proB*-*bsrF* fusion in RMJ13S10 conferred DCS resistance, rather than another element of the amplified region in that suppressor mutant (Fig. 2B). To verify that the altered BsrF protein is responsible, we also tested strains with and without the plasmid carrying  $\Delta$ SS-*bsrF*. As predicted, resistance to DCS increased when  $\Delta$ SS-*bsrF* was expressed, while the shuttle vector alone or carrying wild-type *bsrF* had no effect (Fig. 4B).

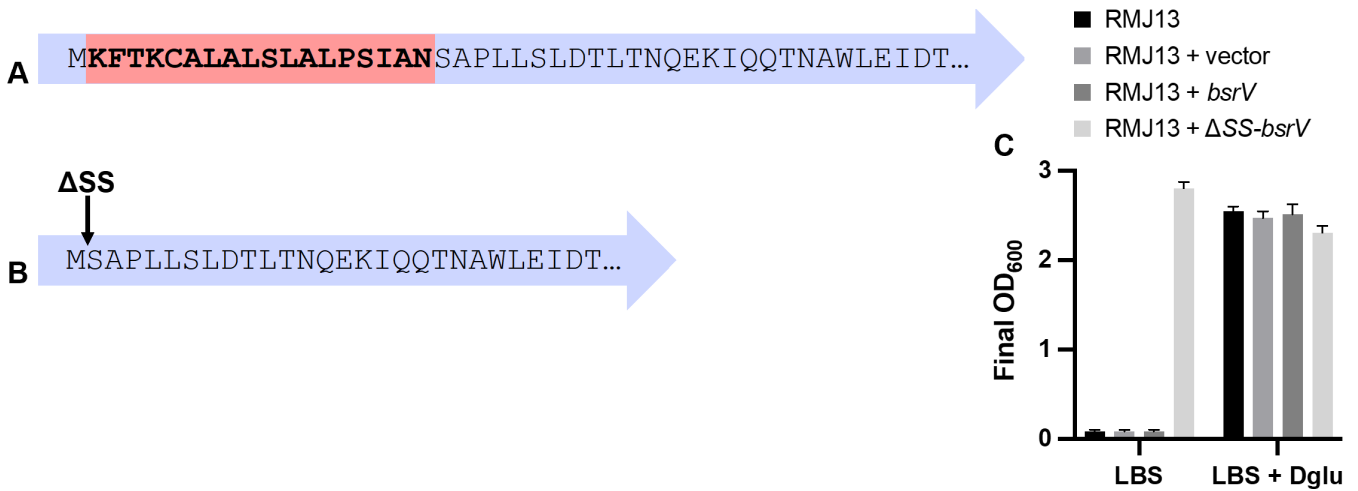


**FIG 3** Schematic of N-terminus of BsrF, with (A) and without (B) the putative Sec-dependent signal sequence. (A) N-terminal amino acid sequence of BsrF; signal sequence that was removed in Δ*SS*-BsrF is highlighted in red. (B) N-terminal amino acid sequence of BsrF that has been altered to remove the signal sequence. New junction is marked with an arrow. (C) Removing the secretion signal from BsrF rescues RMJ13 (*murl::mini-Tn5-erm*) from D-glu auxotrophy. Shown are final OD<sub>600</sub> readings for *V. fischeri* cultures grown with or without 2.7 mM D-glu. Strains include RMJ13 alone, or carrying plasmids pVSV105 (parent vector), pKAL6 (*bsrF*), or pMNC26 (Δ*SS-bsrF*). Cultures were grown for 24 hours before reading the final OD<sub>600</sub>. Error bars indicate the standard error of the mean (*n* = 3). Data from one representative experiment are shown.

### Expression of Δ*SS-bsrF* suppresses multiple auxotrophies

Because DCS interrupts cell wall synthesis by competitively inhibiting D-ala:D-ala ligase (DdIA) and Alr (29), and BsrV from *V. cholerae* has alanine racemase activity (19), we speculated that Δ*SS*-BsrF could be compensating for both the loss of D-glu racemase activity and the inhibition of Alr. To test this hypothesis, we engineered a D-ala auxotrophic strain MC13 (Δ*bsrF* Δ*alr*), as well as a strain auxotrophic for both D-glu and D-ala, MC21 (Δ*bsrF* Δ*alr* Δ*murl*). While these strains require the supplementation of D-ala or D-ala and D-glu, respectively, the expression of Δ*SS-bsrF* allows each of them to grow in LBS without D-ala or D-glu supplementation (Fig. 5).

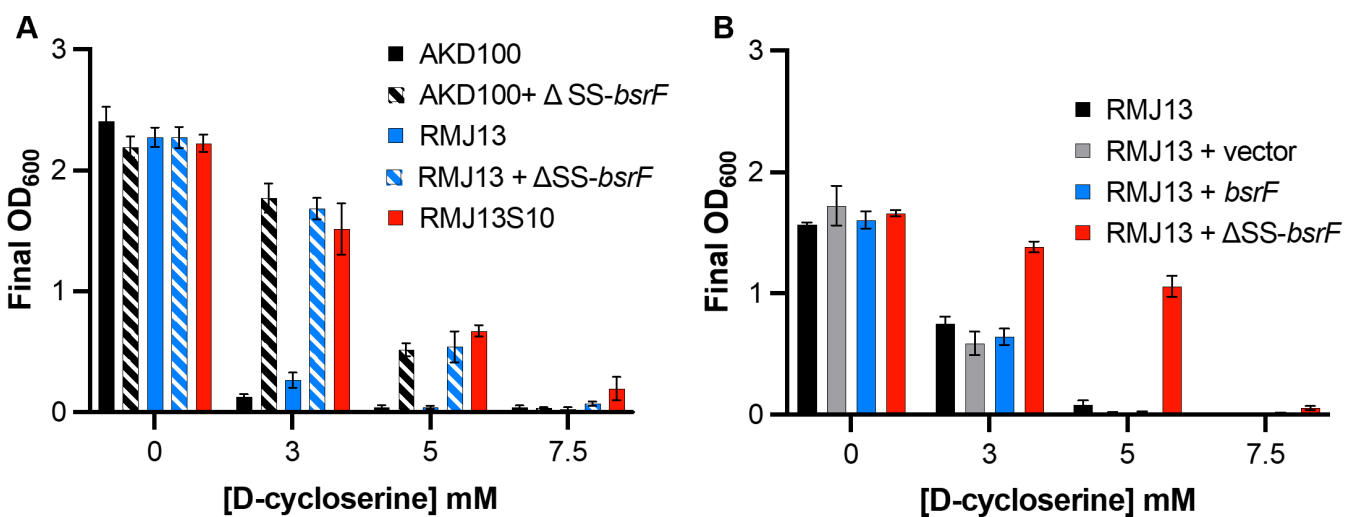


**FIG 4** Removing the secretion signal from BsrF increases resistance to D-cycloserine. (A) Expression of Δ*SS*-BsrF (carried in plasmid pMNC26) increases resistance to DCS in both an Em-resistant derivative of the wild type (AKD100) and the D-glu auxotroph (RMJ13). Similar rescue is seen in RMJ13S10, which has the original *proB-bsrF* fusion. (B) Expression of Δ*SS*-BsrF increases resistance of RMJ13 to DCS, while the empty vector (pVSV105) and WT BsrF (carried in pKAL6) do not. Shown are final OD<sub>600</sub> readings for *V. fischeri* cultures grown with increasing concentrations of DCS. Cultures were grown for 20 (B) or 24 (A) hours before reading OD<sub>600</sub>. Error bars indicate the standard error of the mean (*n* = 6). Data from one representative experiment of at least three are shown.

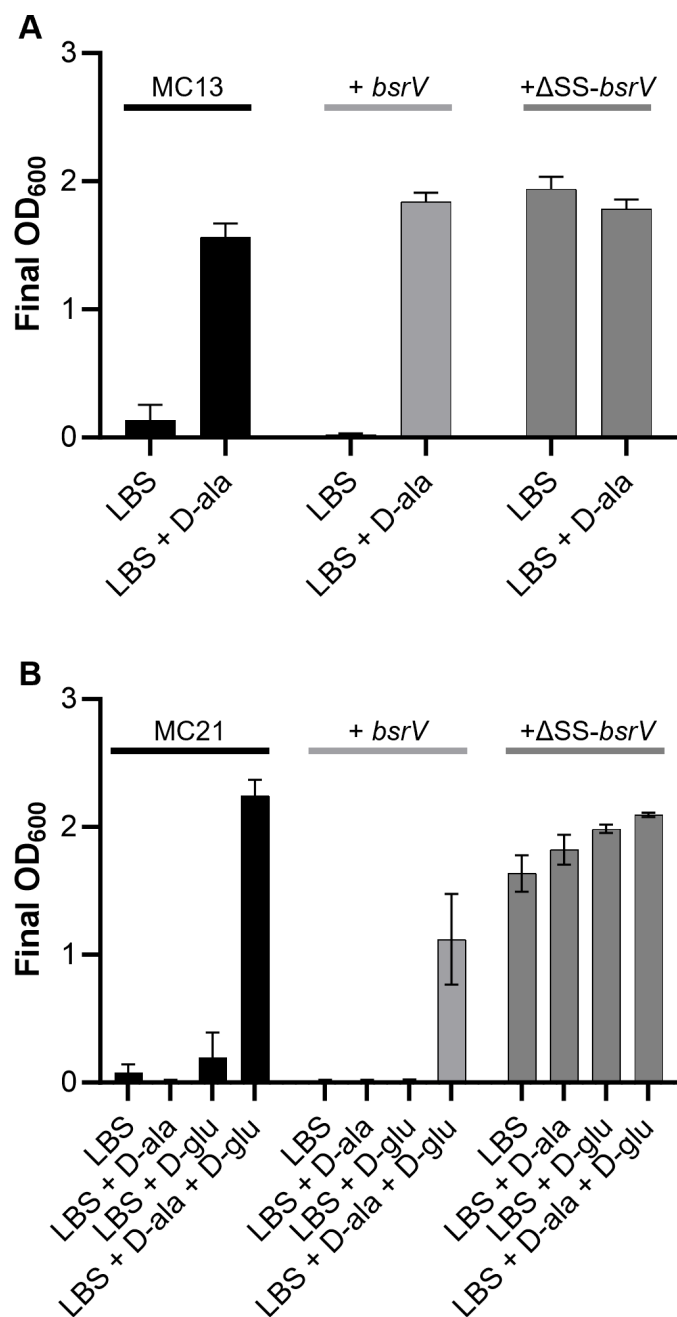


**FIG 5** Removing the secretion signal from BsrF suppresses (A) D-ala auxotrophy and (B) double auxotrophy for D-ala and D-glu. Shown are final OD<sub>600</sub> readings for *V. fischeri* cultures grown in unsupplemented LBS and LBS supplemented with 100  $\mu$ g/mL D-glu and/or D-ala. Strains include MC13 ( $\Delta bsrF \Delta alr::Frt$ ) and MC21 ( $\Delta bsrF \Delta alr::Frt \Delta murI::Frt$ ) alone or carrying plasmids pKAL6 (*bsrF*) or pMNC26 ( $\Delta SS$ -*bsrF*). Cultures were grown for 20 hours before reading OD<sub>600</sub>. Error bars indicate the standard error of the mean ( $n = 4$ ). Data from one representative experiment of at least three are shown.

### The *proB*-*bsrF* and $\Delta SS$ -*bsrF* alleles enable cells to produce PG indistinguishable from the wild type

We speculated that RMJ13S10 and RMJ13 expressing  $\Delta SS$ -*bsrF* would have altered the PG structure because *V. cholerae*'s BsrV does not appear to produce the D-glu that would be needed for D-glu auxotrophs to restore wild-type PG (19). However, D-glu auxotrophs suppressed by the *proB*-*bsrF* fusion and  $\Delta SS$ -*bsrF* have PG that is indistinguishable from

that of wild-type *V. fischeri* (Fig. S1). This was also seen in the strain auxotrophic for both D-ala and D-glu, when suppressed with  $\Delta$ SS-*bsrF* (Fig. S1).

## DISCUSSION

The PG structure is largely structurally conserved throughout the kingdom bacteria, but both structural motifs of PG, the disaccharide strands and peptide chains, do have some natural variation. The glycan strands can have covalent, reversible modifications, usually *N*-deacetylation or *O*-acetylation (30). The amino acids of the peptide chain can also vary to a small extent, based on exogenous factors (31–36) or endogenous factors due to the production of non-canonical amino acids (23, 37, 38). Currently, the only known genetically encoded variations in the PG structure are found in the peptide chain (1, 39). The most common of these variations is the amino acid at the third position, which is *meso*-diaminopimelate (*mDAP*) or L-lys in most bacteria. There are known exceptions that incorporate other diamino acids such as lanthionine and ornithine (40–44) and even rarer cases of monoamino acids (1, 40) into the third position of the peptide chain. Though less common, variations can occur in the first, fourth, and fifth positions of the peptide chain, with structurally similar molecules such as glycine, serine, and lactate replacing the canonical alanine residues (1, 39). Only D-glu is known to be added at the second position of the nascent PG peptide (1), although it may be later modified.

Our approach of selecting suppressors of D-glu auxotrophy parallels similar successful attempts to experimentally evolve PG. Specifically, previous studies, including one in *V. fischeri*, found that the selection of prototrophic suppressors of *mDAP* auxotrophy resulted in the replacement of *mDAP* by lanthionine (37, 45, 46), which is naturally found at this position in *Fusobacterium nucleatum* (41, 42). These results set the precedent and encouraged the current research; however, they focused on the peptide position that has the most natural variation. In contrast, the incorporation of D-glu in the second position of *de novo* PG synthesis is, to the best of our knowledge, invariant. Despite a concerted effort to isolate rare suppressor mutants of D-glu auxotrophy, we did not isolate any mutants that replaced D-glu with another moiety in the PG peptide. For whatever reason(s), D-glu may be a more difficult moiety to replace than DAP.

The lone suppressor mutant selected in this study contained a fusion of *bsrF*, encoding a putative broad-spectrum racemase, onto *proB*, which encodes an enzyme involved in proline and arginine biosynthesis. Further experiments suggested that the ProB moiety was significant only for preventing the secretion of BsrF. Broad-spectrum racemases are being discovered and characterized in a number of bacteria (19, 23, 47–51), and many more are likely unannotated or incorrectly annotated as specific amino acid racemases. However, as appreciation for the production and roles of D-amino acids in bacteria grows, so too does interest in exploring broad-spectrum racemases. Many questions remain as to why bacteria have broad-spectrum racemases and how they are using the non-canonical D-amino acids that are produced.

The best-studied homolog of BsrF is the periplasmic broad-spectrum racemase BsrV in *V. cholerae* (19, 23–27). BsrV can interconvert at least 10 proteinogenic amino acids, as well as 6 non-proteinogenic amino acids, but in the context of this study, it is notably unable to racemize glutamate effectively (19). We found that *V. fischeri* BsrF lacking its putative secretion signal can suppress D-glu auxotrophy by compensating for the loss of Murl and RacD (Fig. 1 and 4), resulting in PG that is indistinguishable from that of the wild type (Fig. S1). Although it is possible that BsrF and  $\Delta$ SS-BsrF have different substrate ranges, SWISS-MODEL predictions suggest that the deletion of the signal sequence has little or no effect on other domains of the protein (data not shown) (52–54). Thus, our results suggest that BsrF can act on glutamate, which would distinguish it from BsrV. Although we cannot rule out the possibility that BsrF generates D-gln, which is then converted to D-glu by another enzyme, the supplementation of LBS with 400  $\mu$ g/mL of D-gln does not restore growth to RMJ13. Future studies will investigate the substrate range for BsrF.

We speculate that BsrF is normally periplasmic and that its racemization activity is, therefore, unable to compensate for the loss of the cytoplasmic Murl in PG biosynthesis. When the secretion signal is removed, BsrF appears to enable sufficient D-glu biosynthesis in the cytoplasm to allow the production of wild-type PG. Similarly, the  $\Delta SS$ -*bsrF* allele compensated for the loss of Alr, suggesting that alanine is also a substrate for BsrF, as it is for BsrV.

If the cytoplasmic BsrF generates other D-amino acids that are not usually produced in the cytoplasm, they appear not to have been incorporated into the PG in significant quantity (Fig. S1). In *V. cholerae*, the activity of BsrV in the periplasm leads to the alteration of the mature PG structure, including the incorporation of D-met at the fifth peptide position (19, 23, 55), so future studies will be aimed at determining whether the same is true for BsrF. Although the *proB*-*bsrF* and  $\Delta SS$ -*bsrF* alleles may lead to the retention of racemase activity in the cytoplasm, a wild-type copy remained even in RMJ13S10, which could potentially support periplasmic function (Fig. 2).

Our results suggest that broad-spectrum racemases might contribute to antimicrobial resistance, with implications for the future development of antimicrobials that target PG and its biosynthesis. We measured the antibiotic resistances of strains expressing wild-type *bsrF* or  $\Delta SS$ -*bsrF*. We focused our studies on antibiotics that disrupt PG synthesis: beta-lactams, vancomycin, and DCS. In contrast to the others, which act on PG crosslinking and remodeling of the mature cell wall, DCS targets cytoplasmic enzymes involved in *de novo* PG synthesis; specifically, DCS inhibits both Alr and DdIA, the enzyme that produces D-ala:D-ala dipeptides for PG biosynthesis (56). Both the  $\Delta SS$ -*bsrF* allele and the *proB*-*bsrF* allele in RMJ13S10 increase resistance to DCS, so we speculate that the enzyme is producing D-ala. Currently, DCS is a second-line antibiotic used for the treatment of infections by multidrug-resistant *Mycobacterium tuberculosis* (57, 58). Although *M. tuberculosis* resistance to DCS is relatively rare, those strains that do arise tend to do so through the mutation of alanine racemase (59). Though different mechanisms for resistance are employed in the two species, the mutation of racemases increased resistance to DCS in both cases.

Though resistance to only one antimicrobial was discovered in this study, the observation that  $\Delta SS$ -BsrF leads to increased resistance to DCS does lead to some concern about antibiotic resistance in pathogens that encode broad-spectrum racemases. Alanine and glutamate racemases have long been targets for antimicrobial drug discovery, due to their essential nature in many bacterial species (17, 57, 60–65). Currently, DCS is the only widely used racemase-inhibiting antimicrobial drug, though the search for more continues. The current research adds to the speculation that these racemase-targeting antibiotics could be rendered impractical by mutation of broad-spectrum racemases (26). Although DCS inhibits Alr, the altered  $\Delta SS$ -BsrF compensates well enough that *V. fischeri* becomes resistant to DCS at levels that would be medically relevant in the treatment of pathogens. Based on the rescue of D-glu auxotrophy, the same possibility could arise against drugs targeting glutamate racemases or the incorporation of D-glu into the growing PG peptide. A serine racemase can confer resistance to the PG-targeting antibiotic vancomycin (66), and the possibility that racemases could underlie additional examples of antimicrobial resistance is concerning, when considering that broad-spectrum racemases and racemases with low specificity are being discovered in primary and opportunistic pathogens (23, 49, 50).

Finally, while unrelated to the goals of this study, the initial finding that the mini-Tn5 disrupting *murl* could spontaneously and precisely delete was important. This phenomenon was also seen when performing similar studies with a mini-Tn5 disruption in *alr* (data not shown). The mini-transposon used in these studies originated from pEV5170 (20), which has been used in many mutagenic analyses of *V. fischeri* (67–75) and other bacteria (76–78), and has been engineered to expand its utility. The reversion rate observed here of about  $10^{-10}$  is sufficiently rare that for most purposes the transposon insertion can be considered stable; however, our results show that with strong selection and a sufficient population, reversion of Tn-disrupted loci can confound an experimental

TABLE 2 Strains and plasmids used in this study<sup>a,b</sup>

| Strain             | Genotype   | Source        |
|--------------------|--|---------------|
| <i>E. coli</i>     |  |               |
| DH5α               | φ80dlacZΔM15 Δ(lacZYA-argF)U169 deoR supE44 hsdR17 recA1 endA1 gyrA96 thi-1 relA1  | (81)          |
| DH5αλpir           | DH5α lysogenized with λpir   | (82)          |
| CC118λpir          | Δ(ara-leu) araD Δlac74 galE galK phoA20 thi-1 rpsE rpsB argE(Am) recA λpir   | (80)          |
| <i>V. fischeri</i> |  |               |
| AKD100             | ES114 with a mini-Tn7-Em   | (83)          |
| ES114              | Wild-type isolate from <i>E. scolopes</i>  | (84)          |
| KL3                | ΔbsrF  | This study    |
| MC9                | ΔbsrF Δalr::Em   | This study    |
| MC13               | ΔbsrF Δalr::FRT  | This study    |
| MC19               | ΔbsrF Δalr::FRT Δmurl::Em  | This study    |
| MC21               | ΔbsrF Δalr::FRT Δmurl::FRT   | This study    |
| RMJ13              | murl::miniTn5-Em ΔracD (VF_1547)   | (18)          |
| RMJ13S10           | murl::miniTn5-Em ΔracD; new amplification junction including bsrF (VF_0375) to proB (VF_0740) [TCCATCGTGATG::TGAAGTTTACTA] | This study    |
| Plasmid            | Relevant characteristics   | Source        |
| pCR-Blunt II-TOPO  | oriV <sub>ColE1</sub> , km <sup>R</sup>  | Thermo Fisher |
| pEV5104            | Conjugative helper plasmid; oriV <sub>R6K</sub> oriT <sub>RP4</sub> km <sup>R</sup>  | (80)          |
| pEV5118            | oriV <sub>R6K</sub> oriT <sub>RP4</sub> cm <sup>R</sup>  | (82)          |
| pKAL4              | bsrF from ES114 cloned into pCR-Blunt II-TOPO  | This study    |
| pKAL6              | bsrF from ES114 cloned into pVSV105  | This study    |
| pKV494             | pJET + FRT-Em <sup>R</sup>   | (85)          |
| pKV496             | pEV579-Kn <sup>R</sup> + flp <sup>+</sup>  | (85)          |
| plostfoX           | tfoX <sup>+</sup> , Cm <sup>R</sup>  | (86)          |
| pMNC26             | ΔSS-bsrF allele cloned into pVSV105  | This study    |
| pRMJ13             | ΔbsrF allele in pCR-Blunt II-TOPO  | This study    |
| pRMJ14             | pRMJ13 ligated to pEV5118  | This study    |
| pVSV105            | oriV <sub>R6K</sub> , oriV <sub>pES213</sub> , oriT <sub>RP4</sub> , cm <sup>R</sup> , lacZα                               | (87)          |

<sup>a</sup>Drug resistance abbreviation used: em, erythromycin; cm, chloramphenicol; Km, kanamycin.

<sup>b</sup>Alleles cloned in this study are from *V. fischeri* strain ES114. Replication origins (*oriV*) on each vector are listed as R6K and/or ColE1. Plasmids based on pES213 are stable in *V. fischeri* and do not require antibiotic selection for maintenance (87).

design. It is, therefore, important to maintain selection for Em, which is encoded on the mini-transposon. This mini-Tn5 lacks a transposase, so we hypothesize that reversion and loss of the mini-Tn5 occur through homologous recombination at the 9 bp direct repeats formed upon insertion.

## MATERIALS AND METHODS

### Bacterial strains and culture conditions

The strains used in this study are listed in Table 2. When added to a lysogeny broth medium (79) for the selection of *Escherichia coli*, chloramphenicol (Cm) and kanamycin (Km) were used at concentrations 20 and 40 μg/mL, respectively. For the selection of *E. coli* with Em, 150 μg/mL was added to a Brain Heart Infusion (BHI) medium (Difco, Sparks, MD). When added to LBS (80) for the selection of *V. fischeri*, Cm, Km, and Em were used at concentrations of 2, 100, and 5 μg/mL, respectively. D-glu and iso-D-gln were added to LBS at a final concentration of 400 μg/mL unless otherwise indicated. The *Fischeri* minimal medium (FMM) [1 mM Tris (pH 7.5), 400 mM NaCl, 10 mM KCl, 50 mM MgSO<sub>4</sub>, 10 mM CaCl<sub>2</sub>, 2 μM FeSO<sub>4</sub>, 2 mM glycerol-3-phosphate, 5 mM ribose, and 20 mM NAG] was used for the natural transformation of *V. fischeri*. In FMM, D-ala and D-glu were added at a final concentration of 25 μg/mL. Agar was added to a final concentration of 1.5% for solid media.

## Molecular genetics and sequence analysis

The plasmids used in this study are listed in Table 2. The oligonucleotides used in this study are listed in Table 3 and were synthesized by Integrated DNA Technologies (Coraville, IA). DNA ligase and restriction enzymes were purchased from New England Biolabs (Beverly, MA). PCR was conducted with KOD DNA polymerase (Millipore Sigma, Burlington, MA). Plasmids used for cloning were prepared with the ZymoPURE Plasmid Miniprep kit (Zymo Research, Irvine, CA). DNA was repurified after PCR and between cloning steps using the DNA Clean & Concentrator kit from Zymo Research. Cloned plasmids were Sanger-sequenced at the University of Illinois–Chicago Genome Research Core facility. Genomic DNA from *V. fischeri* strains was extracted using the Invitrogen PureLink Genomic DNA Mini Kit (Thermo Fisher Scientific, Inc). DNA was then sonicated to generate fragments of approximately 500 bp, and gDNA libraries were prepared using the NEBNext Ultra II DNA library prep kit for Illumina (New England Biolabs), which includes end-repair, adaptor ligation, and addition of index primers. Sequencing was performed by the University of Georgia Genomics and Bioinformatics Core (Athens, GA) on an Illumina NextSeq500 instrument. All sequences were analyzed via Geneious Prime version 2019.0.4 with default settings, and paired-end reads were compared to the reference genome of *V. fischeri* strain ES114.

## Plasmid construction

Plasmids were generated and maintained in *E. coli* DH5 $\alpha$  with the exception of pVSV105 and its derivatives, which were maintained in DH5 $\alpha$ pir, and pEV5104, which was maintained in CC118 $\lambda$ pir (80). When relevant, plasmids were conjugated into *V. fischeri* via triparental mating with helper plasmid pEV5104. Complementation plasmid pKAL6 was constructed by amplifying *bsrF* from ES114 with primers KAL1 and KAL2. This PCR product was cloned into pCR-Blunt II TOPO (Thermo Fisher, Waltham, MA), yielding pKAL4. pKAL4 was then digested with NheI, and the *bsrF*-containing NheI fragment was ligated into XbaI-cut pVSV105 (80) producing pKAL6. Plasmid pMNC26 containing the  $\Delta$ SS-*bsrF* allele was produced by amplifying *bsrF* from pKAL6 with primers MNC23

TABLE 3 Oligonucleotides used in this study

| Primer <sup>a</sup> | Sequence   | Source     |
|---------------------|--|------------|
| Frt-F               | CCA TAC TTA GTG CGG CCG CCT A  | (85)       |
| Frt-R               | CCA TGG CCT TCT AGG CCT ATC CC                                       | (85)       |
| KAL1                | CAT <u>GCT AGC</u> GGT TAA AAA AAC GAC GAT ATA TAA TTC CC            | This study |
| KAL2                | CAT <u>GCT AGC</u> GTA CCT AAT TAT TCT TAC TTA AAT TGG TGC           | This study |
| MNC22               | GGT TAA AAA AAC GAC GAT ATA TAA TTC CC                               | This study |
| MNC23               | GTA CCT AAT TAT TCT TAC TTA AAT TGG TGC                              | This study |
| MNC37               | CAT <u>CCT AGG ACT AGT</u> GTT CTG ATT TGC TTG CTA AAA GTA GTG TCA G | This study |
| MNC38               | CAT <u>CCT AGG CTT ACT</u> TAA ATT GGT GCA ACC CGA CG                | This study |
| MNC43               | CCG TGT TCC CTG CCA ACA ATG  | This study |
| MNC44               | taggcggccgcactaagtatgg CAT AAC TGA AAC CAC AGA CTC                   | This study |
| MNC45               | CCG TGT TCC CTG CCA ACA ATG  | This study |
| MNC46               | ggatagcctagaaggccatgg TAG GAT CAT TAG CAA TAC GCA CTT                | This study |
| MNC50               | CAT <u>CCT AGG</u> AAA CGG TTG TTT ATG TCA GCT CCA CTT CTT TC        | This study |
| MNC51               | GGG CTC GTA TTT CTT CTA CTA TGG GC                                   | This study |
| MNC52               | taggcggccgcactaagtatgg CAT GAT TCA GCC TTA TTA TTC ATC A             | This study |
| MNC53               | ggatagcctagaaggccatgg AAT GAG AGT CTT CTT GAA TTC ATT                | This study |
| MNC54               | CTC TAT ACT CGA GAC ACC GCT ATC                                      | This study |
| RJ14                | GGG TCA TCA TGC AGT AGC GA   | This study |
| RJ28                | AAT <u>GTC GAC</u> CAT AAA CAA CCG TTT TTA TAT AAT AAT TAT TTC G     | This study |
| RJ29                | ATT <u>GTC GAC</u> TAG ACG TCG GGT TGC ACC AAT TTA                   | This study |
| RJ30                | TAA AAA CCG TTT TCA TAA AGG AGA TTC TTG                              | This study |

<sup>a</sup>All oligonucleotides are shown in the 5'-to-3' direction. Underlined regions are restriction enzyme recognition sites. Lowercase bases represent the tail sequences used for splicing fragments via SOE PCR.

and MNC50, which amplify the gene while looping out 54 base pairs of the putative secretion signal sequence. This product was then digested with *AvrII* and ligated into pVSV105 that had been cut with *XbaI* and *SmaI*, yielding pMNC26. To generate a *bsrF*-deletion construct, the ~2-kb region upstream of *bsrF* was PCR-amplified from ES114 using primers RJ14 and RJ28, and the ~1.5-kb region downstream of *bsrF* was amplified with primers RJ29 and RJ30. The upstream and downstream fragments were digested with *Sall*, ligated together, gel-purified, and cloned into pCR-Blunt II TOPO (Invitrogen, Thermo Fisher Scientific, Waltham, MA), to produce pRMJ13. To generate pRMJ14, pRMJ13 was digested with *KpnI* and ligated to *KpnI*-cut pEV5118 (87).

### Construction of mutant strains

Strain KL3 was made via plasmid-mediated allelic exchange, with plasmid pRMJ14. Briefly, a  $\Delta$ *bsrF* allele on plasmid pRMJ14 (described above) was mobilized into ES114 via triparental mating. The resulting  $\Delta$ *bsrF* strain KL3 was verified by PCR with primers MNC22 and MNC23. Additional mutant strains were generated via TfoX-mediated transformation (86). For each, an Em resistance cassette flanked by Frt-recombinase recognition sites was amplified from pKV494 using primers Frt-F and Frt-R. Strain MC9 was made by deleting *alr* from KL3. Briefly, a ~500-bp fragment upstream of *alr* was amplified from ES114 using primers MNC51 and MNC52, and the ~500-bp region downstream of *alr* was amplified with primers MNC53 and MNC54. Fragments were then spliced to either side of the Em cassette splicing by overlap extension PCR (SOE PCR) (85). This fragment was PCR-amplified, then naturally transformed into KL3 carrying the TfoX-overexpressing plasmid plosTfoX (86). Strain MC9 was selected on media containing Em and D-ala. The Em cassette was removed by expressing *flp* recombinase on pKV496 leaving an FLP recombinase recognition site scar in its place, and the plasmid was cured (85). The  $\Delta$ *alr* allele of the resulting strain, MC13, was verified by PCR with primers MNC51 and MNC54. Strain MC19 was then generated by deleting *murl* from MC13. The ~500-bp fragment upstream of *murl* was amplified from ES114 using primers MNC43 and MNC44, and the ~500-bp region downstream of *murl* was amplified with primers MNC45 and MNC46. Fragments were spliced together with Em and amplified as above, then naturally transformed into MC13 carrying the TfoX-overexpressing plasmid plosTfoX. Strain MC19 was selected on media containing Em, D-ala, and D-glu. The Em cassette was again removed by introducing pKV492, screening for loss of the Em marker, and curing the plasmid. The resulting strain, MC21, was verified as  $\Delta$ *murl* by PCR amplification with primers MNC43 and MNC46.

### Selection for spontaneous revertants and suppressor of D-glu auxotrophy

Strain RMJ13 was grown in LBS containing 400  $\mu$ g/mL D-glu (with or without Em, as described above), to an OD<sub>600</sub> of 1. One hundred microliters of culture was plated to LBS without D-glu (in the case of revertants) or LBS containing Em and iso-D-gln (in the case of RMJ13S10). Cultures were dilution-plated non-selectively in parallel on LBS plates supplemented with D-glu, to determine the number of CFU plated and resulting mutation frequency. Plates were incubated at 28°C, and colonies were counted at 24 and 48 hours. Colonies were streak-purified on media containing Em, then frozen at -80°C in LBS with 20% glycerol.

### Mutagenesis of RMJ13 with ethyl methanesulfonate

RMJ13 was grown overnight in 50 mL LBS-Em with 400  $\mu$ g/mL D-glu. The next morning, the strain was subcultured at a 1:500 dilution into 20-mL LBS-Em with D-glu. At an OD<sub>600</sub> between 0.5 and 0.8, cells were harvested by centrifugation at 9,400  $\times$  *g* at room temperature for 5 minutes, then washed twice with 1 M NaCl and centrifuged as before. The pellet was resuspended in 8 mL of minimal medium and split into 4  $\times$  2 mL aliquots. The cultures were incubated shaking at 200 rpm and 28°C for 1 hour. One tube was left untreated; others were dosed with 50  $\mu$ L EMS at 0, 20, or 40 minutes of incubation

(EMS exposure times 60, 40, and 20 minutes, respectively). Cells were harvested by centrifugation as above and washed three times with 1 M NaCl; EMS waste was treated with 10 N NaOH before disposal. Pellets were resuspended in 1 mL of minimal media and incubated shaking at 200 rpm at 28°C. After 5 minutes, 1 mL of minimal media was added to each tube and left to incubate for 10 more minutes. Cells were then plated to LBS-Em without D-glu, for the selection of mutants able to overcome D-glu auxotrophy. Cultures were dilution-plated non-selectively in parallel on LBS-Em supplemented with D-glu, to determine the number of CFU plated and percent killing by EMS. Plates were incubated at 28°C. Colonies were counted at 24 hours; selective plates were incubated for up to 72 hours.

### ***In silico* analyses**

Potential secretion signal sequences in BsrF and the ProB-BsrF fusion were predicted using the SignalP-6.0 server from DTU health (<https://services.healthtech.dtu.dk/services/SignalP-6.0/>) (28), and a probability graph was constructed, with calculated likelihood that the sequences were standard Sec signal peptides, TAT signal peptides, lipoprotein Sec signal peptides, or cleavage sites. Protein similarity scores were analyzed via NCBI services (National Center for Biotechnology Information (NCBI)[Internet]. Bethesda (MD): National Library of Medicine (US), National Center for Biotechnology Information; [2023]—[cited 2017 Apr 06], available from: <https://www.ncbi.nlm.nih.gov/>) and SnapGene software (from Dotmatics; available at [snapgene.com](http://snapgene.com)).

### **Analysis of PG amino acid and muropeptide content**

Cells were grown overnight in LBS with any necessary antibiotics and amino acids, chilled on ice for 10 minutes, and centrifuged at 4°C and 17,600 × *g* for 15 minutes. Pellets were washed by resuspension in 400 mL 1 M NaCl and centrifuged as above. Pellets were resuspended in 10 mL water that had been chilled on ice, then dripped into 50 mL of boiling 4% SDS. The solution was boiled for 30 minutes with continuous stirring and allowed to cool to room temperature, at which point they were centrifuged at 120,000 × *g* for 60 minutes, resuspended in room temperature water, and washed three to four more times by centrifugation and resuspension as above. Before resuspension, the supernatant was assayed for SDS using methylene blue and chloroform (88) and washed repeatedly until no SDS was detected. When SDS was undetectable, the pellet was resuspended in 1 mL of Tris water, then treated with 10 µg DNase I and 50 µg RNase A for 30 minutes at 37°C. Samples were then treated with 100 µg of trypsin, CaCl<sub>2</sub> was added to a final concentration of 10 mM, and samples were incubated overnight at 37°C. Samples were then centrifuged at 15,880 × *g* for 10 minutes, and pellets were resuspended in 1% SDS. The solution was incubated in a 95°C hot water bath for 20 minutes, diluted into warm water, and then centrifuged at 120,000 × *g* for 60 minutes at room temperature. The pellet was then washed with warm water and centrifuged as above, until SDS-free. Subsequent pellets were then resuspended in 12.5 mM NaPO<sub>4</sub> (pH 5.5) and digested with 125 units of Mutanolysin at 37°C overnight. Insoluble material was removed by centrifugation at 15,880 × *g* for 15 minutes. The muropeptide-containing supernatant was transferred to a new tube, lyophilized until dry, and stored at −20°C until analysis. Amino acid (89) and muropeptide (90) analyses were performed using high-pressure liquid chromatography (HPLC) as previously described. Peaks from these analyses were then analyzed by tandem mass spectrometry to further verify the muropeptide structure.

### **ACKNOWLEDGMENTS**

We thank Doreen Nguyen for the technical assistance and Richard Helm at Virginia Tech for performing and analyzing mass spectrometry.

This research was supported by NSF grant IOS-1557964 awarded to E.V.S. and D.L.P.

## AUTHOR AFFILIATIONS

<sup>1</sup>Department of Microbiology, University of Georgia, Athens, Georgia, USA

<sup>2</sup>Department of Biological Sciences, University of Illinois, Chicago, Illinois, USA

<sup>3</sup>Department of Biological Sciences, Virginia Tech, Blacksburg, Virginia, USA

## AUTHOR ORCID*s*

Macey N. Coppinger  <http://orcid.org/0000-0002-0743-873X>

David L. Popham  <http://orcid.org/0000-0002-2614-143X>

Eric V. Stabb  <http://orcid.org/0000-0001-7000-4275>

## FUNDING

| Funder                            | Grant(s)    | Author(s)                        |
|-----------------------------------|-------------|----------------------------------|
| National Science Foundation (NSF) | IOS-1557964 | Eric V. Stabb<br>David L. Popham |

## AUTHOR CONTRIBUTIONS

Macey N. Coppinger, Conceptualization, Formal analysis, Investigation, Methodology, Validation, Writing – original draft, Writing – review and editing | Kathrin Laramore, Formal analysis, Investigation, Validation, Writing – review and editing | David L. Popham, Formal analysis, Funding acquisition, Investigation, Methodology, Project administration, Supervision, Writing – review and editing | Eric V. Stabb, Conceptualization, Formal analysis, Funding acquisition, Methodology, Project administration, Supervision, Writing – original draft, Writing – review and editing

## DATA AVAILABILITY

Illumina reads from whole genome sequencing of ES114 and RMJ13S10 are available in NCBI's Sequence Read Archive (SRA) under accession numbers [SAMN39609062](https://www.ncbi.nlm.nih.gov/sra/SAMN39609062) (ES114) and [SAMN39609073](https://www.ncbi.nlm.nih.gov/sra/SAMN39609073) (RMJ13S10), and all other raw and derived data supporting the findings of this study are available from the corresponding author E.V.S. upon request.

## ADDITIONAL FILES

The following material is available [online](#).

### Supplemental Material

**Figure S1 (JB00333-23-s0001.pdf).** Cytoplasmic BsrF does not affect PG composition.

## REFERENCES

- Vollmer W, Blanot D, de Pedro MA. 2008. Peptidoglycan structure and architecture. *FEMS Microbiol Rev* 32:149–167. <https://doi.org/10.1111/j.1574-6976.2007.00094.x>
- Stabb EV. 2006. The *Vibrio fischeri*-*Euprymna scolopes* light organ symbiosis, p 204–218. In Fabiano LT, Brian A, Jean S (ed), *The Biology of Vibrios*. ASM Press, Washington, DC.
- Stabb EV, Visick KL. 2013. *Vibrio fischeri*: a bioluminescent light-organ symbiont of the bobtail squid *Euprymna scolopes*, p 497–532. In Delong EF, Lory S, Stackebrandt E, Thompson F (ed), *The prokaryotes: Prokaryotic Biology and Symbiotic Associations*, 4th ed. SpringerReference.
- Visick KL, Stabb EV, Ruby EG. 2021. A lasting symbiosis: how *Vibrio fischeri* finds a squid partner and persists within its natural host. *Nat Rev Microbiol* 19:654–665. <https://doi.org/10.1038/s41579-021-00557-0>
- Koropatnick TA, Engle JT, Apicella MA, Stabb EV, Goldman WE, McFall-Ngai MJ. 2004. Microbial factor-mediated development in a host-bacterial mutualism. *Science* 306:1186–1188. <https://doi.org/10.1126/science.1102218>
- Troll JV, Adin DM, Wier AM, Paquette N, Silverman N, Goldman WE, Stadermann FJ, Stabb EV, McFall-Ngai MJ. 2009. Peptidoglycan induces loss of a nuclear peptidoglycan recognition protein during host tissue development in a beneficial animal-bacterial symbiosis. *Cell Microbiol* 11:1114–1127. <https://doi.org/10.1111/j.1462-5822.2009.01315.x>
- Adin DM, Engle JT, Goldman WE, McFall-Ngai MJ, Stabb EV. 2009. Mutations in *ampG* and lytic transglycosylase genes affect the net release of peptidoglycan monomers from *Vibrio fischeri*. *J Bacteriol* 191:2012–2022. <https://doi.org/10.1128/JB.01547-08>
- Goldman WE, Klapper DG, Baseman JB. 1982. Detection, isolation, and analysis of a released *Bordetella pertussis* product toxic to cultured tracheal cells. *Infect Immun* 36:782–794. <https://doi.org/10.1128/iai.36.2.782-794.1982>

9. Melly MA, McGee ZA, Rosenthal RS. 1984. Ability of monomeric peptidoglycan fragments from *Neisseria gonorrhoeae* to damage human fallopian-tube mucosa. *J Infect Dis* 149:378–386. <https://doi.org/10.1093/infdis/149.3.378>
10. Doublet P, van Heijenoort J, Bohin JP, Mengin-Lecreux D. 1993. The *murl* gene of *Escherichia coli* is an essential gene that encodes a glutamate racemase activity. *J Bacteriol* 175:2970–2979. <https://doi.org/10.1128/jb.175.10.2970-2979.1993>
11. Morayya S, Awasthy D, Yadav R, Ambady A, Sharma U. 2015. Revisiting the essentiality of glutamate racemase in *Mycobacterium tuberculosis*. *Gene* 555:269–276. <https://doi.org/10.1016/j.gene.2014.11.017>
12. Brooks JF, Gyllborg MC, Cronin DC, Quillin SJ, Mallama CA, Foxall R, Whistler C, Goodman AL, Mandel MJ. 2014. Global discovery of colonization determinants in the squid symbiont *Vibrio fischeri*. *Proc Natl Acad Sci U S A* 111:17284–17289. <https://doi.org/10.1073/pnas.1415957111>
13. Lyell NL, Septer AN, Dunn AK, Duckett D, Stoudenmire JL, Stabb EV. 2017. An expanded transposon mutant library reveals that *Vibrio fischeri*  $\delta$ -aminolevulinic acid auxotrophs can colonize *Euprymna scolopes*. *Appl Environ Microbiol* 83:e02470-16. <https://doi.org/10.1128/AEM.02470-16>
14. Doublet P, van Heijenoort J, Mengin-Lecreux D. 1992. Identification of the *Escherichia coli murl* gene, which is required for the biosynthesis of D-glutamic acid, a specific component of bacterial peptidoglycan. *J Bacteriol* 174:5772–5779. <https://doi.org/10.1128/jb.174.18.5772-5779.1992>
15. El Zoeiby A, Sanschagrín F, Levesque RC. 2003. Structure and function of the Mur enzymes: development of novel inhibitors. *Mol Microbiol* 47:1–12. <https://doi.org/10.1046/j.1365-2958.2003.03289.x>
16. Mahapatra S, Yagi T, Belisle JT, Espinosa BJ, Hill PJ, McNeil MR, Brennan PJ, Crick DC. 2005. Mycobacterial lipid II is composed of a complex mixture of modified muramyl and peptide moieties linked to decaprenyl phosphate. *J Bacteriol* 187:2747–2757. <https://doi.org/10.1128/JB.187.8.2747-2757.2005>
17. Fisher SL. 2008. Glutamate racemase as a target for drug discovery. *Microb Biotechnol* 1:345–360. <https://doi.org/10.1111/j.1751-7915.2008.00031.x>
18. Jones RM, Popham DL, Schmidt AL, Neidle EL, Stabb EV. 2018. *Vibrio fischeri* DarR directs responses to D-aspartate and represents a group of similar LysR-type transcriptional regulators. *J Bacteriol* 200:e00773-17. <https://doi.org/10.1128/JB.00773-17>
19. Espaillet A, Carrasco-López C, Bernardo-García N, Pietrosevoli N, Otero LH, Álvarez L, de Pedro MA, Pazos F, Davis BM, Waldor MK, Hermoso JA, Cava F. 2014. Structural basis for the broad specificity of a new family of amino-acid racemases. *Acta Crystallogr D Biol Crystallogr* 70:79–90. <https://doi.org/10.1107/S1399004713024838>
20. Lyell NL, Dunn AK, Bose JL, Vescovi SL, Stabb EV. 2008. Effective mutagenesis of *Vibrio fischeri* by using hyperactive mini-Tn5 derivatives. *Appl Environ Microbiol* 74:7059–7063. <https://doi.org/10.1128/AEM.01330-08>
21. Sega GA. 1984. A review of the genetic effects of ethyl methanesulfonate. *Mutat Res* 134:113–142. [https://doi.org/10.1016/0165-1110\(84\)90007-1](https://doi.org/10.1016/0165-1110(84)90007-1)
22. Chen L, Duan L, Sun M, Yang Z, Li H, Hu K, Yang H, Liu L. 2022. Current trends and insights on EMS mutagenesis application to studies on plant abiotic stress tolerance and development. *Front Plant Sci* 13:1052569. <https://doi.org/10.3389/fpls.2022.1052569>
23. Lam H, Oh D-C, Cava F, Takacs CN, Clardy J, de Pedro MA, Waldor MK. 2009. D-amino acids govern stationary phase cell wall remodeling in bacteria. *Science* 325:1552–1555. <https://doi.org/10.1126/science.1178123>
24. Bernardo-García N, Sánchez-Murcia P, Gago F, Cava F, A. Hermoso J. 2016. Structural bioinformatics in broad-spectrum racemases: a new path in antimicrobial research. *Curr Org Chem* 20:1222–1231. <https://doi.org/10.2174/1385272819666150810213115>
25. Cava F. 2017. Divergent functional roles of D-amino acids secreted by *Vibrio cholerae*. *Int Microbiol* 20:149–150. <https://doi.org/10.2436/20.1501.01.296>
26. Aliashkevich A, Alvarez L, Cava F. 2018. New insights into the mechanisms and biological roles of D-amino acids in complex eco-systems. *Front Microbiol* 9:683. <https://doi.org/10.3389/fmicb.2018.00683>
27. Espaillet A, Carrasco-López C, Bernardo-García N, Rojas-Altuve A, Klett J, Morreale A, Hermoso JA, Cava F. 2021. Binding of non-canonical peptidoglycan controls *Vibrio cholerae* broad spectrum racemase activity. *Comput Struct Biotechnol J* 19:1119–1126. <https://doi.org/10.1016/j.csbj.2021.01.031>
28. Nielsen H, Tsigirgos KD, Brunak S, von Heijne G. 2019. A brief history of protein sorting prediction. *Protein J* 38:200–216. <https://doi.org/10.1007/s10930-019-09838-3>
29. Strominger JL, Threnn RH, Scott SS. 1959. Oxamycin, a competitive antagonist of the incorporation of D-alanine into a uridine nucleotide in *Staphylococcus aureus*. *J Am Chem Soc* 81:3803–3804. <https://doi.org/10.1021/ja01523a085>
30. Vollmer W. 2008. Structural variation in the glycan strands of bacterial peptidoglycan. *FEMS Microbiol Rev* 32:287–306. <https://doi.org/10.1111/j.1574-6976.2007.00088.x>
31. Strominger JL, Birge CH. 1965. Nucleotide accumulation induced in *Staphylococcus aureus* by glycine. *J Bacteriol* 89:1124–1127. <https://doi.org/10.1128/jb.89.4.1124-1127.1965>
32. Knüsel F, Nüesch J, Scherrer M, Schmid K. 1967. Effect of lanthionine on the growth of a diaminopimelic acid-heterotrophic mutant of *Escherichia coli*. *Pathol Microbiol (Basel)* 30:871–879.
33. Schleifer KH, Hammes WP, Kandler O. 1976. Effect of endogenous and exogenous factors on the primary structures of bacterial peptidoglycan. *Adv Microb Physiol* 13:245–292. [https://doi.org/10.1016/s0065-2911\(08\)60040-5](https://doi.org/10.1016/s0065-2911(08)60040-5)
34. Mainardi JL, Villet R, Bugg TD, Mayer C, Arthur M. 2008. Evolution of peptidoglycan biosynthesis under the selective pressure of antibiotics in Gram-positive bacteria. *FEMS Microbiol Rev* 32:386–408. <https://doi.org/10.1111/j.1574-6976.2007.00097.x>
35. Tsuruoka T, Tamura A, Miyata A, Takei T, Iwamatsu K, Inouye S, Matsushashi M. 1984. Penicillin-insensitive incorporation of D-amino acids into cell wall peptidoglycan influences the amount of bound lipoprotein in *Escherichia coli*. *J Bacteriol* 160:889–894. <https://doi.org/10.1128/jb.160.3.889-894.1984>
36. Tsuruoka T, Tamura A, Miyata A, Takei T, Inouye S, Matsushashi M. 1985. Second lytic target of beta-lactam compounds that have a terminal D-amino acid residue. *Eur J Biochem* 151:209–216. <https://doi.org/10.1111/j.1432-1033.1985.tb09089.x>
37. Richaud C, Mengin-Lecreux D, Pochet S, Johnson EJ, Cohen GN, Marlière P. 1993. Directed evolution of biosynthetic pathways. Recruitment of cysteine thioethers for constructing the cell wall of *Escherichia coli*. *J Biol Chem* 268:26827–26835.
38. Horcajo P, de Pedro MA, Cava F. 2012. Peptidoglycan plasticity in bacteria: stress-induced peptidoglycan editing by noncanonical D-amino acids. *Microb Drug Resist* 18:306–313. <https://doi.org/10.1089/mdr.2012.0009>
39. Schleifer KH, Kandler O. 1972. Peptidoglycan types of bacterial cell walls and their taxonomic implications. *Bacteriol Rev* 36:407–477. <https://doi.org/10.1128/br.36.4.407-477.1972>
40. Osborn MJ. 1969. Structure and biosynthesis of the bacterial cell wall. *Annu Rev Biochem* 38:501–538. <https://doi.org/10.1146/annurev.bi.38.070169.002441>
41. Kato K, Umemoto T, Sagawa H, Kotani S. 1979. Lanthionine as an essential constituent of cell wall peptidoglycan of *Fusobacterium nucleatum*. *Curr Microbiol* 3:147–151. <https://doi.org/10.1007/BF02601857>
42. Vasstrand EN, Hofstad T, Endresen C, Jensen HB. 1979. Demonstration of lanthionine as a natural constituent of the peptidoglycan of *Fusobacterium nucleatum*. *Infect Immun* 25:775–780. <https://doi.org/10.1128/iai.25.3.775-780.1979>
43. Kato K, Umemoto T, Fukuhara H, Sagawa H, Kotani S. 1981. Variation of dibasic amino acid in the cell wall peptidoglycan of bacteria of genus *Fusobacterium*. *FEMS Microbiol Lett* 10:81–85. <https://doi.org/10.1111/j.1574-6968.1981.tb06211.x>
44. Vasstrand EN, Jensen HB, Miron T, Hofstad T. 1982. Composition of peptidoglycans of Bacteroidaceae: determination and distribution of lanthionine. *Infect Immun* 36:114–122. <https://doi.org/10.1128/iai.36.1.114-122.1982>
45. Consaul SA, Wright LF, Mahapatra S, Crick DC, Pavelka MS. 2005. An unusual mutation results in the replacement of diaminopimelate with lanthionine in the peptidoglycan of a mutant strain of *Mycobacterium*

- smegmatis*. J Bacteriol 187:1612–1620. <https://doi.org/10.1128/JB.187.5.1612-1620.2005>
46. Jones RM, Jr. 2017. Characterization of *Vibrio fischeri* mutants with altered amino acid metabolism and peptidoglycan biosynthesis. Doctor of Philosophy. University of Georgia.
  47. Kino K, Sato M, Yoneyama M, Kirimura K. 2007. Synthesis of DL-tryptophan by modified broad specificity amino acid racemase from *Pseudomonas putida* IFO 12996. Appl Microbiol Biotechnol 73:1299–1305. <https://doi.org/10.1007/s00253-006-0600-6>
  48. Matsui D, Oikawa T, Arakawa N, Osumi S, Lausberg F, Stähler N, Freudl R, Eggeling L. 2009. A periplasmic, pyridoxal-5'-phosphate-dependent amino acid racemase in *Pseudomonas taetrolens*. Appl Microbiol Biotechnol 83:1045–1054. <https://doi.org/10.1007/s00253-009-1942-7>
  49. Miyamoto T, Katane M, Saitoh Y, Sekine M, Homma H. 2017. Identification and characterization of novel broad-spectrum amino acid racemases from *Escherichia coli* and *Bacillus subtilis*. Amino Acids 49:1885–1894. <https://doi.org/10.1007/s00726-017-2486-2>
  50. Radkov AD, Moe LA. 2018. A broad spectrum racemase in *Pseudomonas putida* KT2440 plays a key role in amino acid catabolism. Front Microbiol 9:1343. <https://doi.org/10.3389/fmicb.2018.01343>
  51. Zhao Y, Liu Y, Li N, Muhammad M, Gong S, Ju J, Cai T, Wang J, Zhao B, Liu D. 2022. Significance of broad-spectrum racemases for the viability and pathogenicity of *Aeromonas hydrophila*. Future Microbiol 17:251–265. <https://doi.org/10.2217/fmb-2021-0112>
  52. Guex N, Peitsch MC, Schwede T. 2009. Automated comparative protein structure modeling with SWISS-MODEL and Swiss-PdbViewer: a historical perspective. Electrophoresis 30:S162–S173. <https://doi.org/10.1002/elps.200900140>
  53. Bienert S, Waterhouse A, de Beer TAP, Tauriello G, Studer G, Bordoli L, Schwede T. 2017. The SWISS-MODEL repository-new features and functionality. Nucleic Acids Res 45:D313–D319. <https://doi.org/10.1093/nar/gkw1132>
  54. Waterhouse A, Bertoni M, Bienert S, Studer G, Tauriello G, Gumienny R, Heer FT, de Beer TAP, Rempfer C, Bordoli L, Lepore R, Schwede T. 2018. SWISS-MODEL: homology modelling of protein structures and complexes. Nucleic Acids Res 46:W296–W303. <https://doi.org/10.1093/nar/gky427>
  55. Cava F, de Pedro MA, Lam H, Davis BM, Waldor MK. 2011. Distinct pathways for modification of the bacterial cell wall by non-canonical D-amino acids. EMBO J 30:3442–3453. <https://doi.org/10.1038/emboj.2011.246>
  56. Strominger JL, Ito E, Threnn RH. 1960. Competitive inhibition of enzymatic reactions by oxamycin. J Am Chem Soc 82:998–999. <https://doi.org/10.1021/ja01489a058>
  57. Epstein IG, Nair KG, Boyd LJ. 1955. Cycloserine, a new antibiotic, in the treatment of human pulmonary tuberculosis: a preliminary report. Antibiotic Med Clin Ther (New York) 1:80–93.
  58. de Chiara C, Homšak M, Prosser GA, Douglas HL, Garza-García A, Kelly G, Purkiss AG, Tate EW, de Carvalho LPS. 2020. D-cycloserine destruction by alanine racemase and the limit of irreversible inhibition. Nat Chem Biol 16:686–694. <https://doi.org/10.1038/s41589-020-0498-9>
  59. de Chiara C, Prosser GA, Ogródowicz R, de Carvalho LPS. 2023. Structure of the D-cycloserine-resistant variant D322N of alanine racemase from *Mycobacterium tuberculosis*. ACS Bio Med Chem Au 3:233–239. <https://doi.org/10.1021/acsbiochemau.2c00074>
  60. Azam MA, Jayaram U. 2016. Inhibitors of alanine racemase enzyme: a review. J Enzyme Inhib Med Chem 31:517–526. <https://doi.org/10.3109/14756366.2015.1050010>
  61. Prosser GA, Rodenburg A, Khoury H, de Chiara C, Howell S, Snijders AP, de Carvalho LPS. 2016. Glutamate racemase is the primary target of β-chloro-D-alanine in *Mycobacterium tuberculosis*. Antimicrob Agents Chemother 60:6091–6099. <https://doi.org/10.1128/AAC.01249-16>
  62. Pawar A, Jha P, Konwar C, Chaudhry U, Chopra M, Saluja D. 2019. Ethambutol targets the glutamate racemase of *Mycobacterium tuberculosis*—an enzyme involved in peptidoglycan biosynthesis. Appl Microbiol Biotechnol 103:843–851. <https://doi.org/10.1007/s00253-018-9518-z>
  63. Pawar A, Jha P, Chopra M, Chaudhry U, Saluja D. 2020. Screening of natural compounds that targets glutamate racemase of *Mycobacterium tuberculosis* reveals the anti-tubercular potential of flavonoids. Sci Rep 10:949. <https://doi.org/10.1038/s41598-020-57658-8>
  64. Bongaerts N, Edoz Z, Abukar AA, Song X, Sosa-Carrillo S, Hagenmueller S, Savigny J, Gontier S, Lindner AB, Wintermute EH. 2022. Low-cost antimycobacterial drug discovery using engineered *Escherichia coli*. Nat Commun 13:3905. <https://doi.org/10.1038/s41467-022-31570-3>
  65. Kumar A, Singh E, Jha RK, Khan RJ, Jain M, Varshney S, Muthukumar J, Singh AK. 2023. Targeting multi-drug-resistant *Acinetobacter baumannii*: a structure-based approach to identify the promising lead candidates against glutamate racemase. J Mol Model 29:188. <https://doi.org/10.1007/s00894-023-05587-4>
  66. Stogios PJ, Savchenko A. 2020. Molecular mechanisms of vancomycin resistance. Protein Science 29:654–669. <https://doi.org/10.1002/pro.3819>
  67. Bassis CM, Visick KL. 2010. The cyclic-di-GMP phosphodiesterase BinA negatively regulates cellulose-containing biofilms in *Vibrio fischeri*. J Bacteriol 192:1269–1278. <https://doi.org/10.1128/JB.01048-09>
  68. Miyashiro T, Klein W, Oehlert D, Cao X, Schwartzman J, Ruby EG. 2011. The N-acetyl-D-glucosamine repressor NagC of *Vibrio fischeri* facilitates colonization of *Euprymna scolopes*. Mol Microbiol 82:894–903. <https://doi.org/10.1111/j.1365-2958.2011.07858.x>
  69. Post DMB, Yu L, Krasity BC, Choudhury B, Mandel MJ, Brennan CA, Ruby EG, McFall-Ngai MJ, Gibson BW, Apicella MA. 2012. O-antigen and core carbohydrate of *Vibrio fischeri* lipopolysaccharide: composition and analysis of their role in *Euprymna scolopes* light organ colonization. J Biol Chem 287:8515–8530. <https://doi.org/10.1074/jbc.M111.324012>
  70. Ray VA, Visick KL. 2012. LuxU connects quorum sensing to biofilm formation in *Vibrio fischeri*. Mol Microbiol 86:954–970. <https://doi.org/10.1111/mmi.12035>
  71. Brennan CA, Mandel MJ, Gyllborg MC, Thomasgard KA, Ruby EG. 2013. Genetic determinants of swimming motility in the squid light-organ symbiont *Vibrio fischeri*. Microbiologyopen 2:576–594. <https://doi.org/10.1002/mbo3.96>
  72. Visick KL, Quirk KP, McEwen SM. 2013. Arabinose induces pellicle formation by *Vibrio fischeri*. Appl Environ Microbiol 79:2069–2080. <https://doi.org/10.1128/AEM.03526-12>
  73. Eickhoff MJ, Bassler BL. 2020. *Vibrio fischeri* siderophore production drives competitive exclusion during dual-species growth. Mol Microbiol 114:244–261. <https://doi.org/10.1111/mmi.14509>
  74. Fidopiastis PM, Mariscal V, McPherson JM, McNulty S, Dunn A, Stabb EV, Visick KL. 2021. *Vibrio fischeri* amidase activity is required for normal cell division, motility, and symbiotic competence. Appl Environ Microbiol 87:e02109-20. <https://doi.org/10.1128/AEM.02109-20>
  75. Smith S, Salvato F, Garikipati A, Kleiner M, Septer AN. 2021. Activation of the type VI secretion system in the squid symbiont *Vibrio fischeri* requires the transcriptional regulator TasR and the structural proteins TssM and TssA. J Bacteriol 203:e0039921. <https://doi.org/10.1128/JB.00399-21>
  76. Getz LJ, Thomas NA. 2018. The transcriptional regulator HlyU positively regulates expression of *exsA*, leading to type III secretion system 1 activation in *Vibrio parahaemolyticus*. J Bacteriol 200:e00653-17. <https://doi.org/10.1128/JB.00653-17>
  77. Hu M, Zhang H, Gu D, Ma Y, Zhou X. 2020. Identification of a novel bacterial receptor that binds tail tubular proteins and mediates phage infection of *Vibrio parahaemolyticus*. Emerg Microbes Infect 9:855–867. <https://doi.org/10.1080/22221751.2020.1754134>
  78. Tchelet D, Salomon D. 2022. A rapid fluorescence-based screen to identify regulators and components of interbacterial competition mechanisms in bacteria, p 11–24. In Gal-Mor O (ed), Bacterial Virulence: Methods and Protocols. Springer US, New York, NY.
  79. Miller JH. 1992. A Short Course in Bacterial Genetics: a Laboratory Manual and Handbook for *Escherichia coli* and Related Bacteria. Cold Spring Harbor Laboratory Press, Plainview, N.Y.
  80. Stabb EV, Ruby EG. 2002. RP4-based plasmids for conjugation between *Escherichia coli* and members of the vibronaceae. Methods Enzymol 358:413–426. [https://doi.org/10.1016/s0076-6879\(02\)58106-4](https://doi.org/10.1016/s0076-6879(02)58106-4)
  81. Hanahan D. 1983. Studies on transformation of *Escherichia coli* with plasmids. J Mol Biol 166:557–580. [https://doi.org/10.1016/s0022-2836\(83\)80284-8](https://doi.org/10.1016/s0022-2836(83)80284-8)
  82. Dunn AK, Martin MO, Stabb EV. 2005. Characterization of pES213, a small mobilizable plasmid from *Vibrio fischeri*. Plasmid 54:114–134. <https://doi.org/10.1016/j.plasmid.2005.01.003>
  83. Septer AN, Wang Y, Ruby EG, Stabb EV, Dunn AK. 2011. The haem-uptake gene cluster in *Vibrio fischeri* is regulated by Fur and contributes

- to symbiotic colonization. *Environ Microbiol* 13:2855–2864. <https://doi.org/10.1111/j.1462-2920.2011.02558.x>
84. Boettcher KJ, Ruby EG. 1990. Depressed light emission by symbiotic *Vibrio fischeri* of the sepiolid squid *Euprymna scolopes*. *J Bacteriol* 172:3701–3706. <https://doi.org/10.1128/jb.172.7.3701-3706.1990>
85. Visick KL, Hodge-Hanson KM, Tischler AH, Bennett AK, Mastrodomenico V. 2018. Tools for rapid genetic engineering of *Vibrio fischeri*. *Appl Environ Microbiol* 84:e00850-18. <https://doi.org/10.1128/AEM.00850-18>
86. Pollack-Berti A, Wollenberg MS, Ruby EG. 2010. Natural transformation of *Vibrio fischeri* requires *tfoX* and *tfoY*. *Environ Microbiol* 12:2302–2311. <https://doi.org/10.1111/j.1462-2920.2010.02250.x>
87. Dunn AK, Millikan DS, Adin DM, Bose JL, Stabb EV. 2006. New *rfp*- and pES213-derived tools for analyzing symbiotic *Vibrio fischeri* reveal patterns of infection and *lux* expression *in situ*. *Appl Environ Microbiol* 72:802–810. <https://doi.org/10.1128/AEM.72.1.802-810.2006>
88. Hayashi K. 1975. A rapid determination of sodium dodecyl sulfate with methylene blue. *Anal Biochem* 67:503–506. [https://doi.org/10.1016/0003-2697\(75\)90324-3](https://doi.org/10.1016/0003-2697(75)90324-3)
89. Gonzalez-Castro MJ, Lopez-Hernandez J, Simal-Lozano J, Oruna-Concha MJ. 1997. Determination of amino acids in green beans by derivatization of phenylisothiocyanate and high-performance liquid chromatography with ultraviolet detection. *J Chromatogr Sci* 35:181–185. <https://doi.org/10.1093/chromsci/35.4.181>
90. Popham DL, Helin J, Costello CE, Setlow P. 1996. Analysis of the peptidoglycan structure of *Bacillus subtilis* endospores. *J Bacteriol* 178:6451–6458. <https://doi.org/10.1128/jb.178.22.6451-6458.1996>